The Nature of the β→α″ Transformation in Ti-Nb Alloys

E.M. Hildyard[1], L.D. Connor[2], N. Martin[3], D. Rugg[3], H.J. Stone[1] and N.G. Jones[1*]

1. University of Cambridge, Cambridge, UK

2. Diamond Light Source, Didcott, UK

3. Rolls-Royce plc, Derby, UK

* ngj22@cam.ac.uk

Abstract

The martensitic transformation in Ti-Nb alloys can result in superelastic and shape memory behaviour but significant discrepancies exist between the transformation conditions reported for a given composition. To elucidate the reasons for these variations, *in situ* synchrotron diffraction experiments have been performed on Ti-24Nb (at.%) in two different microstructural conditions. Markedly different transformation behaviour was observed between these two conditions, including fully reversible superelastic behaviour below the apparent martensitic start temperature. These results could not be rationalised using thermally based transformation descriptions. As such, a new approach is introduced based upon the total stress level in a material.

Introduction

Metastable β titanium alloys can exhibit superelastic properties as a result of a martensitic phase transformation, which can occur through a change in temperature, the application of a stress, or a combination of the two. The reversibility and large strains associated with the transformation produce properties that are of interest to the biomedical and aerospace industries [1,2].

Ti-Nb based alloys have been widely studied as they can exhibit both shape memory and superelastic behaviour depending upon both the alloying content [3–8] and the deformation temperature [8–10]. The stability of the β phase is increased by greater Nb contents, suppressing the transformation to the orthorhombic martensite (α″). As such, the corresponding martensite start temperature (M_s) has been reported to be depressed linearly, with a gradient of 43°C for every 1 at.% Nb added [3]. However, there are also reported M_s values that deviate significantly from this trendline [11–14] and, other studies that do not observe a thermally driven β→α″ transformation at all [14–17]. These variations are yet to be fully rationalised but differences in composition, particularly interstitial content [13,18,19], the initial phase constitution [14] and the microstructural condition of a sample [20–23] have all been suggested.

Another potential source of variation between the different studies is the characterisation technique used to determine M_s. Continuous cooling curves [24–26] and differential scanning calorimetry [11,14,27] have often been used to identify key transformation temperatures but these indirect measurement techniques cannot unambiguously identify what is giving rise to recorded signal. Consequently, to provide a better understanding of the β→α″ transformation, there is a need to perform *in situ* experiments that enable a direct measurement of the phase constitution of a sample at specific temperatures and stresses.

Consequently, here we report on the transformation behaviour of a Ti-24Nb (at.%) alloy studied *in situ*, using synchrotron radiation, as a function of temperature. Material was studied in cold rolled and annealed states, revealing markedly different transformation behaviours. The results indicate that the occurrence of a thermally driven β→α″ transformation is highly dependent upon the microstructural condition of the material. An additional elastic load-unload cycle was performed *in situ* on Ti-24Nb (at.%) in the cold rolled condition at –150°C.

Experimental Methods

An ingot of Ti-24Nb (at.%) was arc melted under an argon atmosphere from pure Ti and Nb. Sections of the ingot were cold rolled to a reduction ratio of 90% (equivalent to a final thickness of ~0.6 mm) to refine the grain structure and introduce a high dislocation density into the sample. The samples in the cold rolled condition were heated to 350°C at a rate of 0.5°C/s to remove any α″ that had formed during plastic deformation, and were subsequently cooled to room temperature. This preheated condition of the cold rolled material will be referred to as the CR state.

Tensile specimens, with gauge dimensions of 14 × 0.56 × 0.52 mm, were cut aligned to the rolling direction using electro discharge machining and the resulting re-cast layer was removed through mechanical grinding and polishing. The second microstructural condition was produced by subjecting some of the CR material to a solution heat treatment of 900°C for 5 minutes in an evacuated quartz tube. All of the tubes were water quenched following heat treatment to achieve rapid cooling but were not broken to avoid oxidation during the quench [28]. For consistency, the solution treated samples were also heated to 350°C to remove any α″ that had formed during the quench. This preheated condition of the solution treated material will be referred to as the ST state.

In situ synchrotron X-ray diffraction data, was acquired for the CR and ST specimens using the ID11 beamline at the European Synchrotron Radiation Facility and the I12 beamline at Diamond Light Source. Transmission Debye-Scherrer geometry was employed, using a 0.5 × 0.5 mm monochromatic beam, with wavelengths of 0.15804 and 0.15527 Å respectively. A Linkam TST350 stage was used to (i) cool the ST specimen to -150°C, whilst under a constant load of 2 N and (ii) cool the CR specimen to -150°C, then apply a load/unload tensile cycle to a maximum stress of 300 MPa, followed by a final reheat to 350°C in both cases. A heating and cooling rate of 0.5°C/s and a crosshead movement rate of 1 μm/s were used during these experiments. 2D Debye-Scherrer rings were collected every 4 s and were azimuthally integrated using the Fit2D software [29]. Wavemetrics IGOR Pro was used to fit individual peaks within these 1D datasets using a Gaussian function on a linear background. The peak positions were used to identify the phases present in the microstructure and the normalised peak areas were used as an indicative measure of the phase fraction at each stage during the thermomechanical cycles.

Results

Compositional analysis of the material measured the Nb content of the alloy as 24.2 at.%, with O contents of 0.204 and 0.249 at.% for the CR and ST condition samples respectively. These results indicated that minimal additional oxygen was picked up during the solution heat treatment. Previous studies have reported a suppression in the M_s temperature of 160°C per at.% O in Ti-Nb alloys [4], thus the 0.045 at.% difference measured here would be expected to result in only ~ 7°C variation in M_s between the CR and ST conditions.

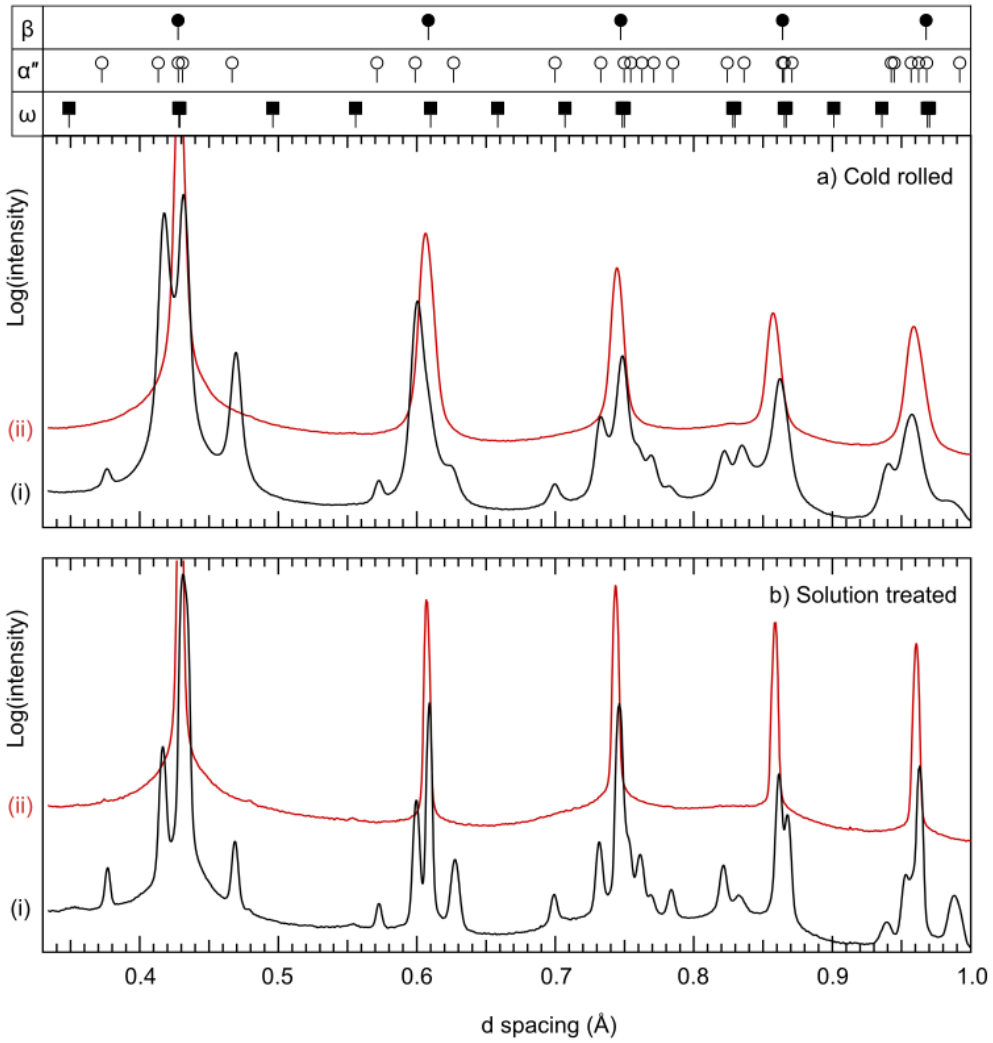

Figure 1: Diffraction patterns for Ti-24Nb in the a) (i) CR condition and (ii) CR at 350°C, and b) the ST condition (i) after quenching and (ii) at 350°C.

Full ring integrated diffraction patterns from the CR state before the initial heat to 350°C, and at 350°C are shown in Figure 1a. Analysis of this data indicated that the CR material contained both the β and α″ phases, with the corresponding peak positions indicated by the markers above the data. The athermal ω phase is also commonly reported in Ti-Nb alloys following rapid cooling and, therefore, the expected reflection positions for this phase are also indicated. Many of the ω and α″ reflections have very similar interplanar spacings, resulting in significant overlap and, therefore, determining whether a small fraction of the ω phase was also present was difficult. At 350°C, the α″ reflections were observed to disappear entirely, leaving a diffraction pattern consisting of β reflections, and slight deviations from the background, which corresponded to ω peak positions.

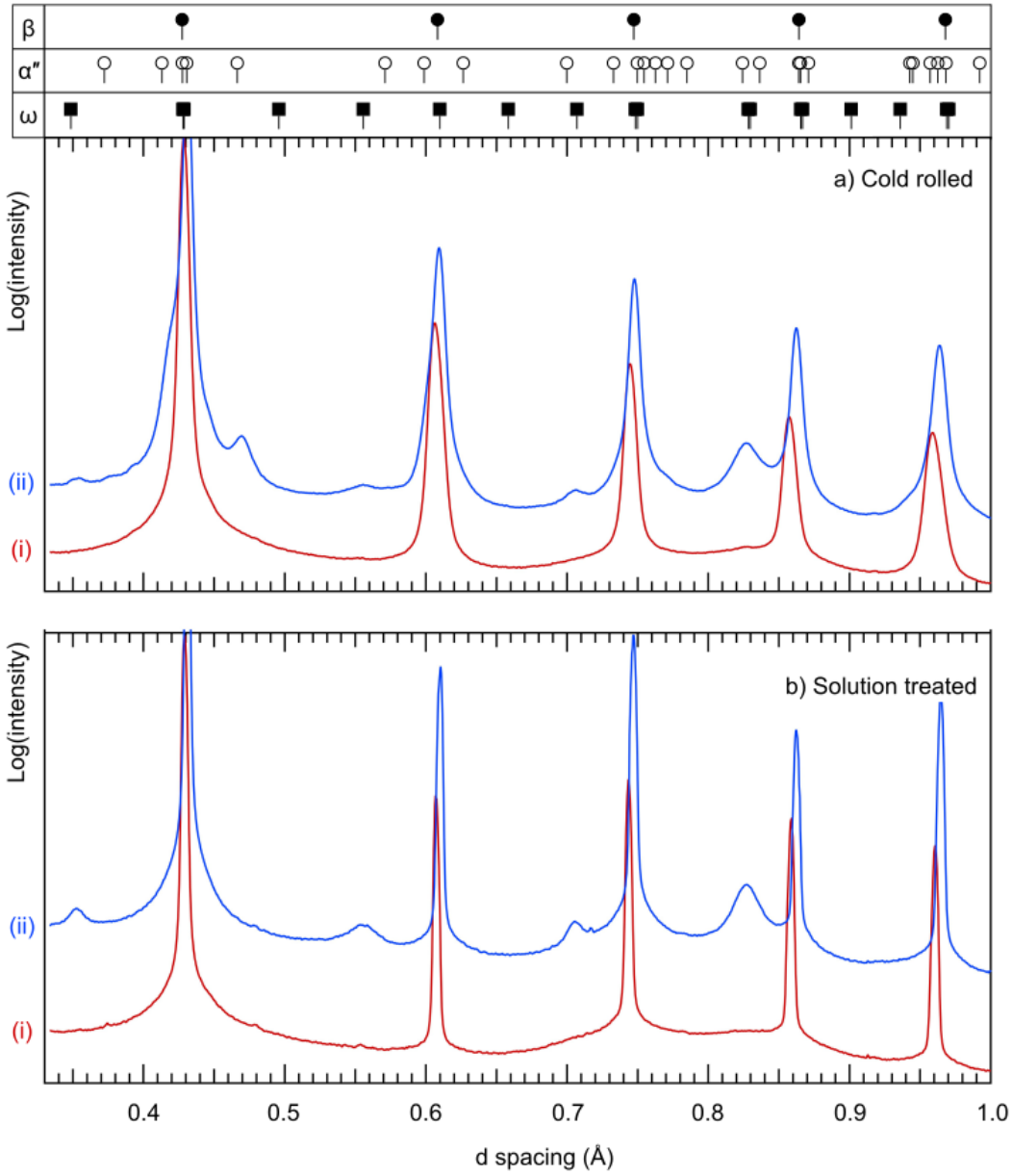

Figure 2: Diffraction patterns for Ti-24Nb in the a) CR condition at (i) 350°C and (ii) -150°C and b) the ST condition at (i) 350°C and (ii) -150°C.

Full ring diffraction patterns for Ti-24Nb after the solution treatment at 900°C for 5 minutes followed by a quench are shown in Figure 1b. Strong peaks that correspond to the β phase were evident along with reflections that were consistent with α″ phase. In addition, very small peaks could also be observed at positions unique to the ω phase. At 350°C, the α″ reflections were observed to disappear entirely, leaving a diffraction pattern consisting of sharp reflections corresponding to the β phase, in addition to very small reflections that were observed at ω peak positions.

The thermally activated transformation behaviour was investigated by cooling both the CR and ST condition material from 350°C to -150°C and the corresponding diffraction patterns are shown in Figure 2. Following cooling, two additional peaks, corresponding to the α″ phase, had appeared in the CR diffraction pattern, suggesting that the β→α″ transformation had occurred. The intensity of the ω peaks had also increased markedly. Critically, no additional α″ reflections were observed in the ST diffraction pattern and the ω reflections had increased similarly to those in the CR condition.

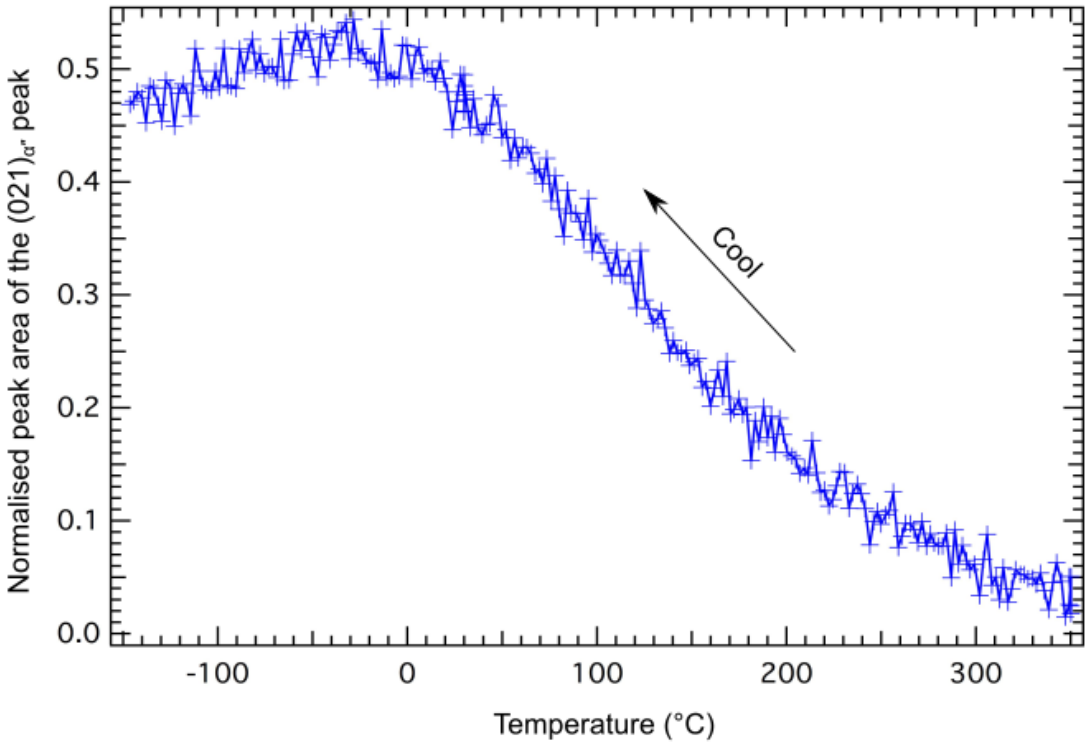

Figure 3: Evolution of the $(021)_{\alpha''}$ peak intensity during cooling from 350°C to -150°C.

To directly determine the transformation temperatures in the CR material, the evolution of the α'' phase as a function of temperature and stress was tracked using the intensity of the $(021)_{\alpha''}$ peak, which had an interplanar spacing that was unique to the α'' phase and located at 0.47 Å in Figure 2. The evolution of the $(021)_{\alpha''}$ peak area, normalised to that of the initial deformed condition in Figure 1a, during cooling to -150°C is shown in Figure 3. The intensity of the $(021)_{\alpha''}$ peak was observed to remain at a background level, until the temperature was decreased below 310°C and the peak area began to increase. This suggested that the M_s temperature for this Ti-24Nb alloy was ~310°C, more than 200°C higher than previously reported values [12,14,27]. As the temperature was further reduced, the $(021)_{\alpha''}$ peak area continued to increase until a temperature of 0°C was reached, at which point no additional increase in intensity was observed with further cooling and the peak area reached a plateau. This observation is surprising and is not in line with conventional understanding of thermally driven martensite formation, where the transformation would be expected to proceed towards completion and a fully martensitic structure [19,30].

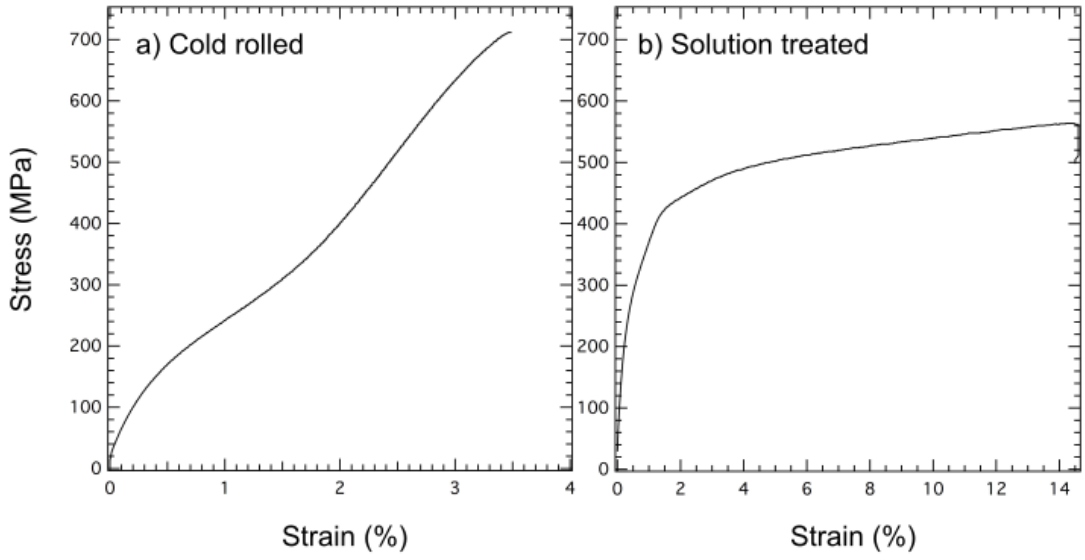

Figure 4: Room temperature stress-strain curves to failure for Ti-24Nb in the a) CR, and b) ST conditions, after the initial heat to 350°C.

The stress-strain curves of the CR and ST conditions are shown in Figure 4. It is generally expected that when a superelastic alloy is subjected to an external load, the strain response at low stresses follows linear elastic deformation. However, the stress-strain curve of the CR material, Figure 4a, did not exhibit a linear elastic response at any point. Instead, the gradient of the stress-strain curve began to bend as soon as an external load was applied. Since the CR material at room temperature is expected to have contained

an initial volume fraction of both the β and α″ phases, this curve could be either attributed to the occurrence of the β→α″ transformation or the reorientation of the original α″ variants. The transformation region continued with increasing stress until the sample fractured at ~700 MPa.

In contrast the stress-strain response of the ST material, Figure 4b, showed an initial linear elastic response up to a stress of ~150 MPa. Above this applied stress level, the stress-strain response began to curve, indicating that the stress-induced β→α″ transformation had initiated. Unlike the initial phase constitution of the CR condition, the diffraction data for the ST condition showed no evidence for the α″ phase, enabling the non-linear elastic behaviour to be attributed to the occurrence of the β→α″ transformation. The transformation region continued with increasing stress until the macroscopic yield point was reached, at a stress of ~400 MPa.

To provide more insight into the transformation behaviour behind the non-linear deformation exhibited by the CR material, a load-unload tensile test to a maximum stress of 300 MPa was performed *in situ*. Figure 5 shows the fitted $(021)_{\alpha''}$ peak area, normalised to that of the initial deformed condition, during the thermomechanical cycle with a loading temperature of -150°C. After the initial cool, which has already been discussed in Figure 3, the CR condition material was subjected to an externally applied load. As soon as a load was applied, the $(021)_{\alpha''}$ peak area was observed to immediately increase, suggesting that the critical stress required to drive the transformation was < 4 MPa, which provides an explanation for the lack of a linear elastic region in Figure 4a.

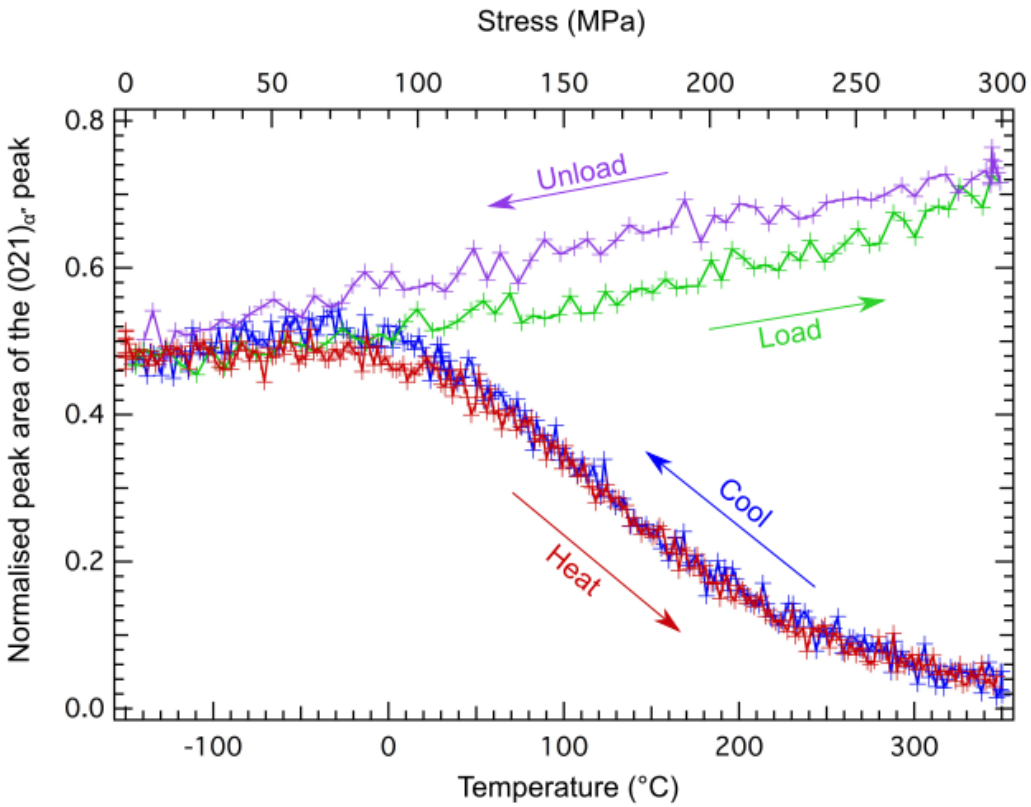

Figure 5: Evolution of the $(021)_{\alpha''}$ peak intensity during cooling to -150°C and loading to 300 MPa, followed by removal of the load, and a final heat to 350°C.

More significantly, the reverse behaviour occurred during the unloading segment of the thermomechanical cycle, shown by the intensity of the $(021)_{\alpha''}$ peak decreasing as the magnitude of the applied stress was reduced. Furthermore, upon the complete removal of the applied stress, the intensity of the $(021)_{\alpha''}$ peak was found to have the same magnitude as it did prior to loading. This dataset suggested that a reverse transformation had occurred with the α″ phase reverting to the parent β phase, and, that all of the α″ phase, which formed as a result of the macroscopically applied stress, was fully reversible. Critically, these observations cannot be rationalised by current critical temperature based transformation theories, which imply that the α″ variants would not change when unloaded below M_s [31]. Upon reheating to 350°C, the intensity of the $(021)_{\alpha''}$ peak followed a non-linear behaviour identical to that observed during the initial cool from 350°C to -150°C.

Discussion

The results presented here conclusively show that microstructural condition has a pronounced effect of the β→α″ transformation. CR condition material formed α″ when cooled below ~310°C, whereas ST condition material did not form α″, despite being cooled to -150°C. Since, there was no appreciable compositional difference between the conditions, the differences in behaviour must be a consequence of microstructural condition, for example, the size of the parent β grains, the presence of the ω phase and the dislocation density in the material. These observations are in contrast with current temperature based transformation theories that imply that the transformation temperatures are dominated by the composition of an alloy.

Additionally, current theories would imply that if an alloy is subjected to a load-unload cycle below M_s, it cannot undergo the reverse α″→β transformation upon unloading as there is no thermodynamic driving force. Thus, the evidence presented here, showing a reverse transformation in CR material when unloaded at -150°C, significantly below

the apparent M_s temperature of ~310˚C, cannot be rationalised. As such, the combination of these two results means that the true M_s temperature for this composition must be below -150°C.

One possible explanation for these observations is that the change in Gibbs energy with stress is sufficiently large that the β→α″ transformation occurs once a critical stress level, for a given temperature, has been reached. Importantly, this critical stress is not simply associated with an applied load, but is the total stress within a material, which can have multiple contributions, both internal and external. The internal stresses may arise from thermal mismatches between grains or phases (Type II stresses) and from features within the microstructure, such as dislocations (Type III stresses). If the sum of these contributions locally exceeds the critical transformation stress, then the relative values of the Gibbs energies change and the β→α″ martensitic transformation becomes favourable.

This new stress based mechanism was further validated by the observation of the full superelastic recovery of the CR material when subjected to a load-unload cycle at -150°C. The immediate increase in the $(021)_{\alpha''}$ peak area as soon as the external load was applied suggested that at -150°C, the magnitude of the internal stress level of the CR material must have been lying just below the value for the critical stress required for transformation. The observation of the plateau region between 0°C and -150°C suggested that this may also have been the case at temperatures below 0°C, another observation that could not be rationalised using current thermally driven transformation theories.

Conclusions

The influence of microstructural condition on the transformation behaviour of Ti-24Nb has been studied using *in situ* synchrotron diffraction. CR material was observed to form α″ on cooling below ~310˚C, whilst ST material did not transform upon cooling to -150˚C. In addition, fully reversible superelastic behaviour was observed in CR material tested at -150˚C. As such, the M_s temperature for this composition must be < -150°C. These results can be rationalised using existing thermally based transformation descriptions and, thus, a new stress based approach had been defined.

References

[1] T. Duerig, A. Pelton, D. Stöckel, Mater. Sci. Eng. A 273–275 (1999) 149–160

[2] W. Cai, Y.F. Zheng, X. Meng, L.C. Zhao, Mater. Sci. Forum. 475–479 (2005) 1915–1920

[3] H.Y. Kim, H. Satoru, J. Il Kim, H. Hosoda, S. Miyazaki, Mater. Trans. 45 (2004) 1090–1095

[4] J. Il Kim, H.Y. Kim, H. Hosoda, S. Miyazaki, Mater. Trans. 46 (2005) 852–857

[5] S. Miyazaki, H.Y. Kim, H. Hosoda, Mater. Sci. Eng. A 438–440 (2006) 18–24

[6] H.Y. Kim, J. Fu, H. Tobe, J. Il Kim, S. Miyazaki, Shape Mem. Superelasticity. 1 (2015) 107–116

[7] H.Y. Kim, S. Miyazaki, Y. Ikuhara, J. Il Kim, H. Hosoda, Mater. Trans. 56 (2015) 625–634

[8] H.Y. Kim, S. Miyazaki, Shape Mem. Superelasticity. 2 (2016) 380–390

[9] Y. Al-Zain, H.Y. Kim, T. Koyano, H. Hosoda, S. Miyazaki, Scr. Mater. 103 (2015) 37–40

[10] H.Y. Kim, J. Il Kim, T. Inamura, H. Hosoda, S. Miyazaki, Mater. Sci. Eng. A 438–440 (2006) 839–843

[11] H. Matsumoto, S. Watanabe, S. Hanada, Mater. Trans. 46 (2005) 1070–1078

[12] W. Elmay, F. Prima, T. Gloriant, B. Bolle, Y. Zhong, E. Patoor, P. Laheurte, J. Mech. Behav. Biomed. Mater. 18 (2013) 47–56

[13] M. Tahara, T. Inamura, H.Y. Kim, S. Miyazaki, H. Hosoda, Scr. Mater. 112 (2016) 15–18

[14] M. Bönisch, A. Panigrahi, M. Calin, T. Waitz, M. Zehetbauer, W. Skrotzki, J. Eckert, J. Alloys Compd. 697 (2017) 300–309

[15] Y. Mantani, M. Tajima, Mater. Sci. Eng. A 438–440 (2006) 315–319

[16] E. Lopes, A. Cremasco, C. Afonso, R. Caram, Mater. Charact. 62 (2011) 673–680

[17] A. Nyayadhish, B. Maji, M. Krishnan, Proc. Int. Conf. Martensitic Transform. ICOMAT-08. (2009) 493–497

[18] J. Il Kim, H.Y. Kim, T. Inamura, H. Hosoda, S. Miyazaki, Mater. Sci. Eng. A 403 (2005) 334–339

[19] P. Castany, A. Ramarolahy, F. Prima, P. Laheurte, C. Curfs, T. Gloriant, Acta Mater. 88 (2015) 102–111

[20] X. Ma, W. Sun, J. Alloys Compd. 509 (2011) 294–298

[21] F. Sun, S. Nowak, T. Gloriant, P. Laheurte, A. Eberhardt, F. Prima, Scr. Mater. 63 (2010) 1053–1056

[22] B. Sun, X.L. Meng, Z.Y. Gao, W. Cai, L.C. Zhao, J. Alloys Compd. 715 (2017) 16–20

[23] F. Sun, Y. Hao, S. Nowak, T. Gloriant, P. Laheurte, F. Prima, J. Mech. Behav. Biomed. Mater. 4 (2011) 1864–1872

[24] Y. Huang, S. Suzuki, H. Kaneko, T. Sato, Sci. Technol. Appl. Titan. (1970) 691–693

[25] K. Jepson, A. Brown, J. Gray, Sci. Technol. Appl. Titan. (1970) 677–690

[26] T. Sato, H. Seikiti, Y.C. Huang, J. Aust. Inst. Met. 5 (1960) 149

[27] Y. Al-Zain, H.Y. Kim, H. Hosoda, T.H. Nam, S. Miyazaki, Acta Mater. 58 (2010) 4212–4223

[28] E.L. Pang, MPhil Thesis, University of Cambridge, 2016

[29] A.P. Hammersley, S.O. Svensson, A. Thompson, Nucl. Inst. Methods Phys. Res. A. 346 (1994) 312–321

[30] L. Héraud, P. Castany, D. Lailllé, T. Gloriant, Mater. Today Proc. 2 (2015) S917–S920

[31] K. Yamauchi, Ohkata, Tsuchiya, S. Miyazaki, Shape memory and superelastic alloys: technologies and applications, 2011